Atmos. Chem. Phys., 17, 8395–8410, 2017
https://doi.org/10.5194/acp-17-8395-2017

Atmospheric Chemistry and Physics
Open Access
EGU

Seasonal cycle of desert aerosols in western Africa: analysis of the coastal transition with passive and active sensors

Habib Senghor[1], **Éric Machu**[1,2], **Frédéric Hourdin**[3], **and Amadou Thierno Gaye**[1]

[1]Laboratoire de Physique de l'Atmosphère et de l'Océan Siméon-Fongang (LPAO-SF), École Supérieure Polytechnique (ESP) de l'Université Cheikh Anta Diop (UCAD), Dakar, Senegal
[2]Laboratoire d'Océanographie Physique et Spatiale (LOPS), IUEM, Université Brest, CNRS, IRD, Ifremer, Brest, France
[3]Laboratoire de Météorologie Dynamique (LMD), CNRS/IPSL/UMPC, Paris, France

Correspondence to: Habib Senghor (habib.senghor@ird.fr)

Received: 28 July 2016 – Discussion started: 6 December 2016
Revised: 29 April 2017 – Accepted: 29 May 2017 – Published: 11 July 2017

Abstract. The impact of desert aerosols on climate, atmospheric processes, and the environment is still debated in the scientific community. The extent of their influence remains to be determined and particularly requires a better understanding of the variability of their distribution. In this work, we studied the variability of these aerosols in western Africa using different types of satellite observations. SeaWiFS (Sea-Viewing Wide Field-of-View Sensor) and OMI (Ozone Monitoring Instrument) data have been used to characterize the spatial distribution of mineral aerosols from their optical and physical properties over the period 2005–2010. In particular, we focused on the variability of the transition between continental western African and the eastern Atlantic Ocean. Data provided by the lidar scrolling CALIOP (Cloud-Aerosol Lidar with Orthogonal Polarization) onboard the satellite CALIPSO (Cloud Aerosol Lidar and Infrared Pathfinder Satellite Observations) for the period 2007–2013 were then used to assess the seasonal variability of the vertical distribution of desert aerosols. We first obtained a good representation of aerosol optical depth (AOD) and single-scattering albedo (SSA) from the satellites SeaWiFS and OMI, respectively, in comparison with AERONET estimates, both above the continent and the ocean. Dust occurrence frequency is higher in spring and boreal summer. In spring, the highest occurrences are located between the surface and 3 km above sea level, while in summer the highest occurrences are between 2 and 5 km altitude. The vertical distribution given by CALIOP also highlights an abrupt change at the coast from spring to fall with a layer of desert aerosols confined in an atmospheric layer uplifted from the surface of the ocean. This uplift of the aerosol layer above the ocean contrasts with the winter season during which mineral aerosols are confined in the atmospheric boundary layer. Radiosondes at Dakar Weather Station (17.5° W, 14.74° N) provide basic thermodynamic variables which partially give a causal relationship between the layering of the atmospheric circulation over western Africa and their aerosol contents throughout the year. A SSA increase is observed in winter and spring at the transition between the continent and the ocean. The analysis of mean NCEP (National Centers for Environmental Prediction) winds at 925 hPa between 2000 and 2012 suggest a significant contribution of coastal sand sources from Mauritania in winter which would increase SSA over the ocean.

1 Introduction

The Sahara is the largest source of mineral aerosols in the world, with a contribution of almost 40 % compared to the overall emissions from natural sources (Ramanathan et al., 2001; Tanaka et al., 2005). The mineral dust aerosols emitted from the Sahara can be transported over long distances in the atmosphere and can be detected in locations as far as the Americas (Prospero et al., 1981; Swap et al., 1992; Formenti et al., 2001; Kaufman et al., 2005; Ansmann et al., 2009; Ben-Ami et al., 2010), the Mediterranean region (Bergametti et al., 1989; Moulin, 1997; Ansmann et al., 2003), and Asia (Ganor and Mamane, 1982; Israelevich et al., 2003; Ganor et al., 2010). However, here the study of dust transport focuses on the main corridor of their transport westward of

Africa (Formenti et al., 2001). The aerosols play a very important role on the climate and the various processes involved in the climate system (Kaufman et al., 2005; Teller and Levin, 2006; Stith et al., 2009) through their direct impact in the visible, infrared (Sokolik and Toon, 1999), and the earth radiation budget (Andreae, 1996; Solomon, 2007), which is still poorly understood. The difficulty of understanding the impact of aerosols on the Earth's radiation balance is due to the large spatial and temporal variability of their concentration and composition in the atmosphere. The mineral particles suspended in the atmosphere come from different sources and have a nature similar to that of the soil from which they arise (Claquin et al., 1999; Formenti et al., 2008) with a broad spectrum of particle sizes ranging between 0.01 and 300 µm (Wagener, 2008; Ryder et al., 2013). Their impact on the marine ecosystem and particularly on oceanic primary production (Duce and Tindale, 1991; Baker et al., 2003; Mills et al., 2004; Jickells et al., 2005; Mahowald et al., 2009) still remains uncertain and difficult to assess because of the composition of these particles and of physicochemical processes affecting them (e.g., Friese et al., 2016). Mineral dust deposition also has a negative impact on human health and are responsible for meningitis epidemics and cardiac diseases (Thomson et al., 2006; Martiny and Chiapello, 2013; Diokhane et al., 2016; Prospero et al., 2005; Griffin, 2007).

Although the transport of mineral dust across the Atlantic Ocean started to be investigated in the 1960s, it only started to be studied from satellite observations in the 1970s (Kaufman et al., 2005; Taghavi and Asadi, 2008). Passive sensors have the advantage of providing daily data on the state of the atmosphere with good spatial and temporal coverage. The satellite products have improved our knowledge of the source regions and dust transport pathways in recent years (Engelstaedter et al., 2006; Schepanski et al., 2007, 2009b, 2012). However, studies of their spatial and temporal variability are mainly based on indices such as the aerosol optical depth (AOD) or the aerosol index (AI), which provide vertically integrated information on the atmospheric aerosol contents (passive space-derived observations: Cakmur et al., 2001; Chiapello and Moulin, 2002; Kaufman et al., 2005; Engelstaedter et al., 2006; Schepanski et al., 2009b). Moreover AOD estimated by satellite integrates the contribution of every kind of particle, and this latter estimation also depends on the altitude at which aerosols are located. Based on perturbations induced by the Rayleigh scattering in the detection of absorbing aerosols, Chiapello et al. (1999) showed that TOMS AI is more sensitive to aerosols present at high altitude than at low altitude. In other words the signal changes with the height of the aerosol plume depending on aerosol content.

Recently, the vertical structure of the Saharan air layer (SAL) has been analyzed from CALIPSO satellite observations. The vertical discontinuity of dust layers between land and ocean strongly impacts the atmospheric deposition rates of mineral matter (Schepanski et al., 2009a) and dust concentration at the oceanic surface, which has important consequences on the primary biological productivity of surface waters (Martin, 1992; Arístegui et al., 2009).

In boreal summer, SAL is characterized by hot, dry, very dust-laden air, and it is located between 10 and 25° N (Dunion and Marron, 2008; Tsamalis et al., 2013). This SAL is marked by very strong potential temperatures up to 40 °C and a radon presence (^{222}radon) indicating the desert origin of air masses (Carlson and Prospero, 1972).

In winter, the SAL is characterized by the transport of dust containing chemical elements such as aluminum (Al), silicon (Si), iron (Fe), titanium (Ti), and manganese (Mn; e.g., Formenti et al., 2001; Ben-Ami et al., 2010) and is located between 5 and 10° N (e.g., Tsamalis et al., 2013). Some studies relating aerosols to their transport are generally a simple description of the vertical distribution of aerosols in the SAL (Generoso et al., 2008; Liu et al., 2008; Ben-Ami et al., 2009; Braun, 2010; Yu et al., 2010; Adams et al., 2012; Ridley et al., 2012; Yang et al., 2012) or a description of the seasonality of the SAL in connection with large-scale dynamics (Liu et al., 2012; Tsamalis et al., 2013). However, the dust field campaigns, AMMA, SAMMUM-1 and SAMMUM-2, FENNEC, and SALTRACE (see Table 1) of Weinzierl et al. (2016) carried out in western Africa and over the Atlantic Ocean improved our understanding of dust–dynamics interactions. During SALTRACE, a linear depolarization ratio of particles and a relative humidity threshold of 50 % were used for differentiating different types of aerosol (Weinzierl et al., 2016). Authors showed that sea salt aerosol were restricted to the lower layer superposed by biomass–dust mixtures. They also showed that the altitude of the mineral dust layer decreased westward. The effects of small-scale dynamics and thermodynamics for controlling the vertical structure of desert aerosols in coastal western Africa remain unknown, and efforts made in this direction are restricted to very sporadic case studies (Gamo, 1996; Reid et al., 2002; Petzold et al., 2011).

In this study, in situ and satellite observations are used to describe the seasonal timescale of mineral dust distribution. We first used complementary information, provided by SeaWiFS and OMI which deliver extensive (AOD) and intensive single-scattering albedo (SSA) and Ångström exponent (AE) parameters of desert aerosols, to analyze the spatial variability of the desert aerosol dust. Then we used CALIOP lidar onboard CALIPSO to investigate the vertical distribution of these desert aerosols.

We finally analyze meteorological data to explain the impact of the atmospheric variables on the seasonal cycle of the vertical distribution of desert aerosols at the transition zone between the continent and the ocean. We conclude the present work by summarizing all the results which are reflecting our common knowledge on mineral dust discrimination and spatiotemporal distribution.

2 Methodology and data

2.1 AErosol RObotic NETwork (AERONET)

We first used data of AOD from AERONET between January 2005 and December 2010. AERONET is a global network of in situ observations developed by the NASA Earth Observing System (NASA EOS) (Dubovik et al., 2000). AERONET consists of the CIMEL solar photometers providing measures of AOD every 15 min, refractive index and also allows inversions such as particle size distribution of aerosols and SSA at 440, 670, 870, and 1020 nm wavelengths (Holben et al., 1998) with an accuracy of ± 0.01 (Eck et al., 1999; Dubovik et al., 2000; Holben et al., 2001). This uncertainty is inherent in the algorithm inversion used to retrieve aerosol characteristics. Some approximations are used in the numerical inversion algorithm which produce errors named relative errors having a standard deviation of 0.01 (Dubovik et al., 2000). AERONET's SSAs are computed for favorable atmospheric conditions (AOD 440 nm > 0.4 and solar zenith angle $> 45°$) using an algorithm which performs almucantar inversions (Jethva et al., 2014). These data are used to validate remotely sensed AOD and SSA measurements. AERONET is available in three different products: Level 1.0, 1.5, and 2.0. In this study, we use Level 1.5 product for the Cabo Verde station, due to a lack of sufficient Level 2 data, and Level 2.0 for the other stations. Concerning the temporal resolution of AERONET observations, we compute a "daily" mean based upon data collected between 10:00 and 15:00 in order to use observations collected during the same time window as satellite overpass. We then use this 10:00–15:00 daily averages to compute monthly 10:00–15:00 AOD.

2.2 Sea-viewing Wide Field-of-view Sensor (SeaWiFS)

We then used DeepBlue-SeaWiFS monthly mean AOD at 550 nm and AE products derived from SeaWiFS developed by NASA to study ocean color. SeaWiFS measures the solar radiation reflected at the top of the atmosphere in the wavelengths 412, 443, 490, 510, 555, 670, 765, and 865 nm. Satellite measurements carried out between October 1997 and December 2010 (Jamet et al., 2004; Hsu et al., 2012) have a value of signal to noise and uncertainty of 2–3 % for the different spectral bands (for details see Eplee et al., 2007; Franz et al., 2007; Eplee Jr. et al., 2011). In this paper, we use the Level 3 version 4 products (Bettenhausen and Team, 2013) for years 2005 to 2010. The SeaWiFS AOD provided at 550 nm is available both over the land and over the ocean (Hsu et al., 2004; Sayer et al., 2012). The products used here are land–ocean estimates generated and made available to the scientific community by NASA (Wang et al., 2000). Regarding the contribution of the aerosol types in the AOD, the studies of Dubovik et al. (2002), Schepanski et al. (2009b) or Tegen et al. (2013) suggested that the coarse-mode fraction of mineral dust dominates the atmospheric mixture when AE values, associated with AOD values greater than or equal to 0.3, are below 0.7.

Here, we consider aerosols optical thickness larger than 0.2 when the Ångström exponent is lower than 0.7 (Fig. 4) to monitor the evolution of coarse (upper and lower bounds, respectively) and fine (lower and upper bounds) modes of mineral aerosols.

2.3 Ozone Monitoring Instrument (OMI)

OMI is a passive sensor onboard the Aura satellite launched on 15 July 2004 by NASA EOS Aura spacecraft which released its first observations in October 2004. Like all satellites in the A-Train constellation, OMI scans the entire Earth in 14 to 15 orbits with a nadir ground pixel spatial resolution of $13\,\text{km} \times 24\,\text{km}$ (Jethva et al., 2014). In addition to the ozone content in the atmosphere OMI provides information on aerosols, clouds, gases (NO_2, SO_2, HCHO, BrO, and OClO), and irradiance in the ultraviolet (Levelt et al., 2006). We use Aura/OMI SSA at 500 nm (taken from https://ozoneaq.gsfc.nasa.gov/data/lance-browse/) and the OMAERUV Level 3 Collection 003 aerosol product processed in March 2012 with a spatial resolution of $1° \times 1°$ to quantify the scattering of the aerosol types with passive sensors. The OMAERUV algorithm assigns a flag to each pixel which carries information on the quality of the retrieval (Jethva et al., 2014).

The SSA represents the ratio (ranging between 0 and 1) of scattering coefficient to extinction coefficient and provides information about the absorbing properties of the aerosols. SSA of 0.9 indicates that 90 % of the total extinction of solar light is caused by scattering and 10 % by absorption effects (Jethva et al., 2014). This parameter depends on the wavelength, size, and the complex refractive index of particles (Léon et al., 2009). The closer this value is to one the more desert aerosols dominate (Johnson et al., 2008; Léon et al., 2009; Ialongo et al., 2010; Malavelle, 2011).

OMI data were interpolated on the grid of SeaWiFS data to superimpose the products (AOD and SSA).

2.4 Cloud Aerosol Lidar and Infrared Pathfinder Satellite Observations (CALIPSO)

The first polarization lidar in space, CALIPSO, is a sun-synchronous satellite developed by NASA as part of the Earth System Science Pathfinder program (ESSP) and launched on 28 April 2006 (Winker et al., 2007; Hunt et al., 2009) in order to provide global coverage of the vertical distribution of the properties of clouds and aerosols (Winker, 2003). The CALIOP lidar onboard CALIPSO acquires vertical profiles of the atmosphere at 30 m resolution in the lower layers (from the two orthogonal components that result from depolarization of a signal backscattered laser at 532 nm and vertical profiles of a total laser at 1064 nm signal backscattered at nadir). The final Level 2 product is reduced to a

uniform resolution calculated from averaging and/or interpolating different resolutions for generating intermediate products (Winker et al., 2006). We use the Vertical Feature Mask (VFM; stage 1, version 3) for which the processing algorithm is described in CALIOP Algorithm Theoretical Basis, Part 3: Scene Algorithms Classification (Liu et al., 2005). VFM allows to separate aerosols from clouds but also the desert aerosols from other types of aerosols (Omar et al., 2009). This methodology of discrimination by CALIOP of aerosol types gives results close to another method of distinction between mineral dust made from inversions (SSA and AE) of AERONET Level 2 products (Mielonen et al., 2009). The mix of layers of desert aerosol and other types of aerosols (i.e., biomass burning) is very rare (Chou et al., 2008; Heese and Wiegner, 2008) in our region of interest. During the dry season, mineral aerosols are observed in the atmospheric surface layer ranging 0.5 to 1 km while the aerosols emitted through biomass burning are carried to higher levels, up to 5 km altitude (Cavalieri et al., 2010). Nevertheless, classification errors are possible for low values of the mineral dust occurrence frequency (MDOF) and at frontal zones between layers of different substances (Adams et al., 2012). For this reason we only consider here the values of MDOF above 10 %. Our method for determining the mineral dust by a calculation of the MDOF is equivalent to Adams et al. (2012) and follows the equation

$$p(x,y,z) = \frac{\sum_{n=0}^{N} p(x+n,y,z)}{\sum_{n=0}^{N} s(x+n,y,z)} \quad \forall \quad x,y,z, \qquad (1)$$

where p is the frequency of occurrence of dust at a grid point, s the total number of valid satellite passing the same grid point, and N the total number of grid points. The occurrences in the longitude (x) are summed and normalized by the total valid satellite passes in a given longitudinal range (35° W–20° E). Data were gridded with a near-uniform horizontal resolution of $0.5° \times 0.5°$ and a vertical resolution of 30 m for 290 vertical levels between 0.5 and 8.2 km above sea level. The CALIOP lidar on CALIPSO (also in the A-Train) has a 90 m instantaneous footprint which is smeared to 333 m in the along track direction by orbital motion over the lidar pulse duration. All satellites of the A-Train constellation, such as CALIPSO, fly in a sun-synchronous orbit with a 16-day coverage cycle consisting of 233 orbits separated by 1.54° longitude or about 172 km at the Equator. Each satellite completes 14.55 orbits per day with a separation of 24.7° longitude between each successive orbit at the Equator. These CALIPSO orbits are controlled to cover the same ground with cross-track errors of less than ±10 km (Winker et al., 2007). This drastically reduces the spatial coverage of the satellite. Consequently, we use a mesh of 0.5° longitude to cover the area between 10–24° W and 12–21° N. The choice of this band of latitude is driven by one of the objectives of the paper which is to study the transition of aerosol distribution between the continent and the ocean. Dust occurrences are averaged over latitudes 12 to 21° N and are then smoothed over the 30-point longitudinal running mean and 50-point vertical running mean.

3 Results

3.1 Horizontal dust distribution

SeaWiFS AOD (estimated at wavelength 550 nm) represents an average value of the optical depth of the atmosphere. It has first been compared to the monthly AOD given by AERONET photometers (given at the wavelength 675 nm and interpolated at 550 nm) by calculating the correlation between the two measurements at different selected stations (Fig. 1). Our choice focused on the stations Banizoumbou (2.665° E–13.541° N), Agoufou (1.479° W–15.345° N), M'bour (16.959° W–14.394° N), and Cabo Verde (22.935° W–16.733° N) to assess the quality of satellite information obtained across the land–ocean continuum. A very good correlation is calculated between SeaWiFS and in situ measurement given by the photometer at Banizoumbou ($R = 0.97$; Fig. 1a). The CIMEL photometer at Agoufou (Mali) also shows a very good correlation with SeaWiFS ($R = 0.87$; Fig. 1b). The correlation between the two measures is equal to 0.81 at the shore in M'bour (Fig. 1c). It is close to the one in Cabo Verde ($R = 0.83$; Fig. 1d). All these correlation values of AOD are significant at 95 % using the Student statistical test. The regression for M'bour site is not as good as for the other sites. This site is located at the shore, at the interface between land and ocean, and the satellite algorithm retrieval is not the same over the land and over the ocean. We also studied the structure of the cloud of points between the two data sets to assess the quality of the satellite measurements as a function of the aerosol concentration. The regression line obtained by the least squares method shows a linear relationship between satellite and in situ monthly mean measurements of AOD at the selected stations.

The horizontal transport of desert aerosols can be followed by considering the key and complementary parameters that distinguish them. To better characterize the desert aerosols, we combined AOD (SeaWiFS) with SSA (OMI) to specify the contribution of the latter compared to other types of aerosols in the atmosphere. A threshold of 0.90 in monthly averaged SSA is used to define regions dominated by desert aerosols. This value is chosen in agreement with the threshold value given in previous studies (Léon et al., 2009; Malavelle, 2011; Jethva et al., 2014). This method allowed us to define the Saharan and Sahelian as the one which is the most influenced by dust plumes composed of desert aerosols throughout the year (between 12 and 21° N; Fig. 3).

The comparison of the daily SSA of Aura/OMI versus AERONET is achieved to validate satellite SSA which provides a better spatiotemporal coverage of our region of interest. OMI SSA retrievals are taken between 10:00 and 15:00,

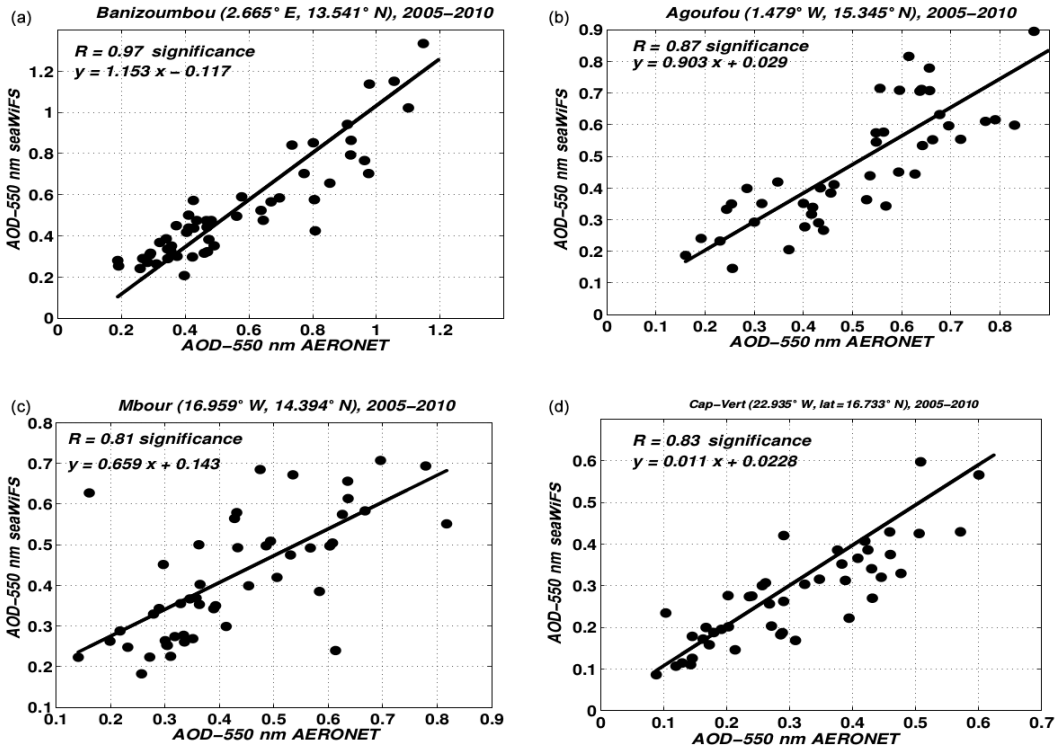

Figure 1. Comparison of monthly mean aerosol optical depth (AOD) between SeaWiFS (550 nm) and ground measurements from AERONET (675 nm) from January 2005 to December 2010. This comparison is done at the following stations: **(a)** Banizoumbou (53 points), **(b)** Agoufou (47 points), **(c)** M'bour (50 points), and **(d)** Cabo Verde (47 points). The black solid line represents the regression between both data sets.

which covers AERONET measurements. As emphasized by Jethva et al. (2014), this comparison is done at the original wavelengths of each independent measurement (388 nm for OMI and 440 nm for AERONET) in order to avoid uncertainties induced by the interpolation at other wavelengths. Good correlations are retrieved between the two data sets at the different ground stations in western Africa for the period 2005–2010 within root mean square difference (RMSD) of 0.03 in the selected region (Fig. 2). Globally, the OMAERUV SSA is well correlated with ground measurements. The correlation at all selected sites for this study is significant. The agreement between the two inversions is better over the continent (Banizoumbou station, $r = 0.47$ and Agoufou station: $r = 0.50$) and at the shore of western Africa (M'bour station: $r = 0.66$) than over the ocean (Cabo Verde station: $r = 0.30$). The discrepancy between the AERONET SSA retrievals over continental (Banizoumbou and Agoufou) and coastal western Africa (M'bour) was already found by Johnson and Osborne (2011) during the GERBILS campaign over western Africa. These authors suggested that a lack of sampling may affect the results. Their results are in agreement with our results which show 449 retrievals in Banizoumbou against 178 retrievals in M'bour site.

Figure 3 shows a seasonal distribution of the AOD which is superimposed onto SSA in the western African region. Both large AOD and strong SSA indicate that mineral dust is the dominant component of aerosols in the atmosphere. In winter, the main dust source in western Africa, the Bodélé depression, is showed in Fig. 3a with AOD larger than 0.5 and SSA larger than 0.9 around 17° N–18° E. This most persistent dust hotspot is activated all along the year and provides a maximum dust emission in spring (Fig. 3b), in agreement with Engelstaedter and Washington (2007). In summer, the intense surface heating from solar radiation (heat low) induces the development of a near-surface thermal low pressure system over northern Mali, southern Algeria, and eastern Mauritania (Lavaysse et al., 2009; Messager et al., 2010) and controls the dry convective processes which contribute to about 35 % of the global dust budget (Engelstaedter and Washington, 2007). Over the northwestern Sahara region (Fig. 3c), the AOD is larger than 0.5 and SSA is stronger than 0.9, both variables indicate the main hotspot of mineral dust source in western Africa in summer which has already been shown by Engelstaedter and Washington (2007).

Figures 3 and 4 show that horizontal monthly average of AOD is stronger above the continent than over the ocean throughout the year. The weakest AOD is given for winter months (DJF for December–January–February) with a mean value of 0.33 ± 0.07 (standard deviation). At this season, the SSA values are higher in the northeast tropical Atlantic than

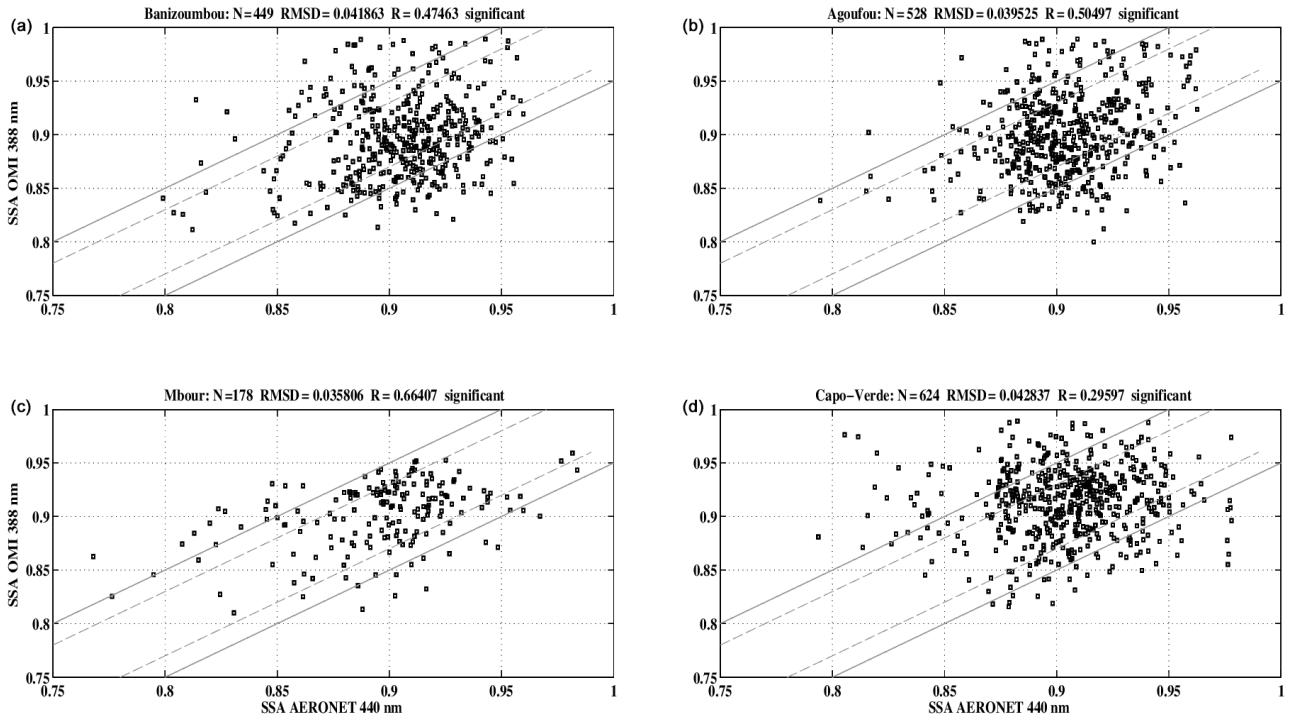

Figure 2. OMAERUV SSA at 388 nm wavelength as a function of AERONET SSA at 440 nm at **(a)** Banizoumbou (2.66° E, 13.54° N; 449 retrievals); **(b)** Agoufou (1.47° W, 15.34° N; 528 retrievals); **(c)** M'bour (16.95° W, 14.39° N; 178 retrievals); and **(d)** Cabo Verde (22.93° W, 16.73° N; 624 retrievals). The solid lines indicate the domain where the two retrievals agree with each other within 0.03 and the dashed lines indicate agreement within 0.05.

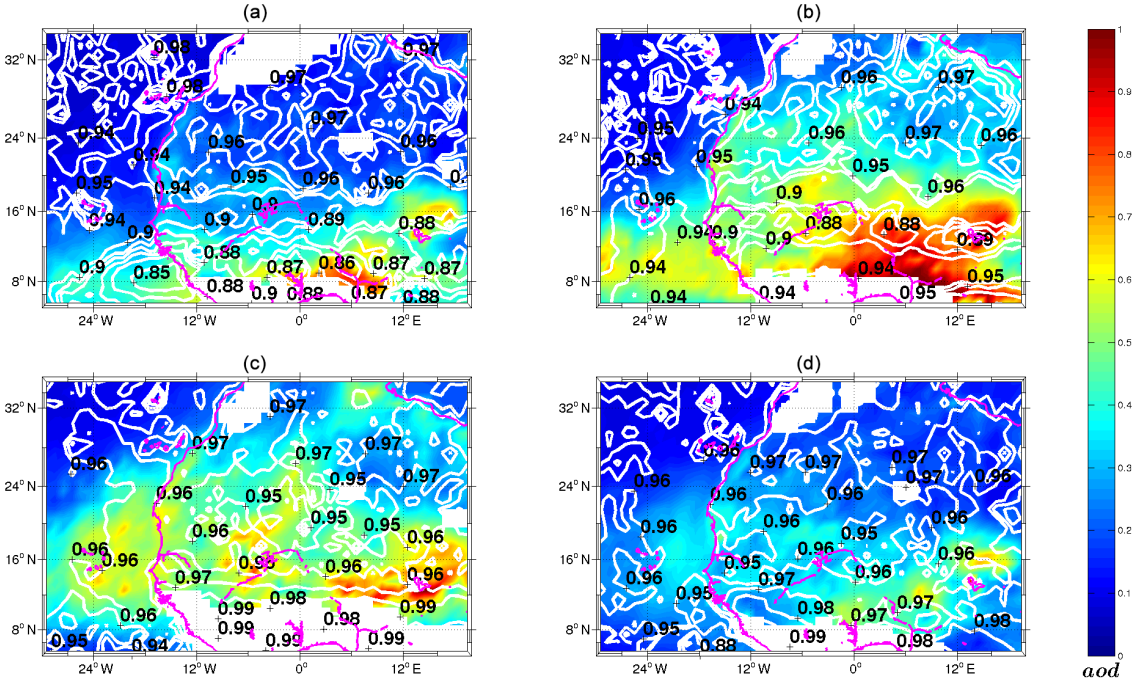

Figure 3. Seasonal distribution of aerosol optical depth (average between 2005 and 2010) at 550 nm wavelength (colors) from SeaWiFS for **(a)** DJF; **(b)** MAM; **(c)** JJA; and **(d)** SON. SSA from OMI is superimposed with white contour lines.

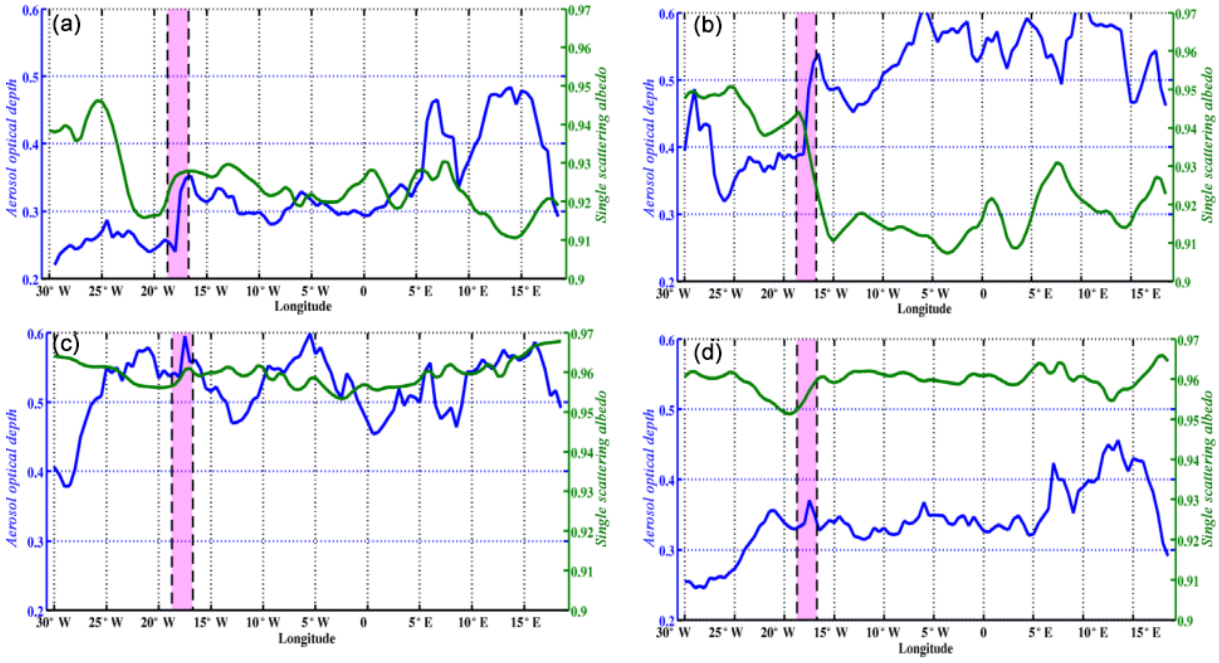

Figure 4. Seasonal SeaWiFS AOD at 550 nm (blue), Aura/OMI SSA (green) zonally averaged between 12 and 21° N and from 2005 to 2010: **(a)** DJF; **(b)** MAM; **(c)** JJA; and **(d)** SON. The black dashed lines indicate the continent–ocean transition for the latitude range 12–21° N.

on continental western Africa with a SSA maximum reaching 0.95. This indicates a stronger contribution of dust over the ocean than over the continent in the latitude range 12–21° N. Note that sources of dust aerosols are also indicated by high SSA values north of 21° N. The air masses advection in the lower atmosphere (925 hPa) follows a northeast–southwest direction in winter (Fig. 6a), dust coming from the northwest of Mauritania is partially seen over the continent (in AOD and SSA), and its main signature should be seen over the ocean. In spring (MAM for March–April–May), the increase of the monthly mean AOD compared to winter is indicated by a stronger mean value (0.50 ± 0.08). The mean optical depth indicates that the dust sources are becoming more active with an atmosphere more charged than in winter. The coarse mode dominates in the mixed atmosphere boundary layer over the continent with lower values of AE less than 0.7 (not shown). Nevertheless, the reflectance properties of aerosols (given by the SSA) is higher over the ocean than over the continent and vary weakly compared to winter.

In summer (JJA for June–July–August), the maximum mean AOD is 0.52 ± 0.05. AOD values are associated with higher SSA above 0.96. It indicates that aerosols are clearly dominated by desert dust in boreal summer. At this season, important quantities of dust can be lifted up and vertically transported in the upper atmosphere by convective systems and near-surface convergence (Engelstaedter and Washington, 2007).

In autumn (SON for September–October–November), the monthly mean AOD is 0.34 ± 0.05. AOD is decreased compared to spring but the SSA values are much higher than in spring despite the fact that uplift occurrences are larger in spring than in fall in western Africa (Marticorena et al., 2010; Diokhane et al., 2016).

Changes of AOD and SSA are seen at the transition between the continent and the ocean (Fig. 4). Understanding these changes requires a thorough analysis of the vertical distribution of dust during transportation from east to west in northern Africa.

3.2 Vertical dust distribution

The vertical distribution of desert aerosol indicates a strong presence of dust concentrations between the surface and 6 km in agreement with the results of Léon et al. (2009), who studied the vertical distribution of dust in the northeast tropical Atlantic (Fig. 5).

In DJF, desert aerosols are mainly concentrated in the atmospheric boundary layer (ABL) between the surface and 2 km (Fig. 5a) both over the continent and the ocean. At this season, we also noted a homogeneous dust aerosol transition between western Africa and the eastern part of the Atlantic Ocean.

In MAM, there is an elevation of the SAL with a maximum altitude of 5 km on the continent and between 4 and 5 km above the ocean (Fig. 5b). The MDOF over 50 % above the continent shows that dust emissions are much greater than in winter. The ABL develops vertically to reach up to 5 km of altitude. It results in an atmospheric layer well mixed between the surface and 5 km of altitude above the conti-

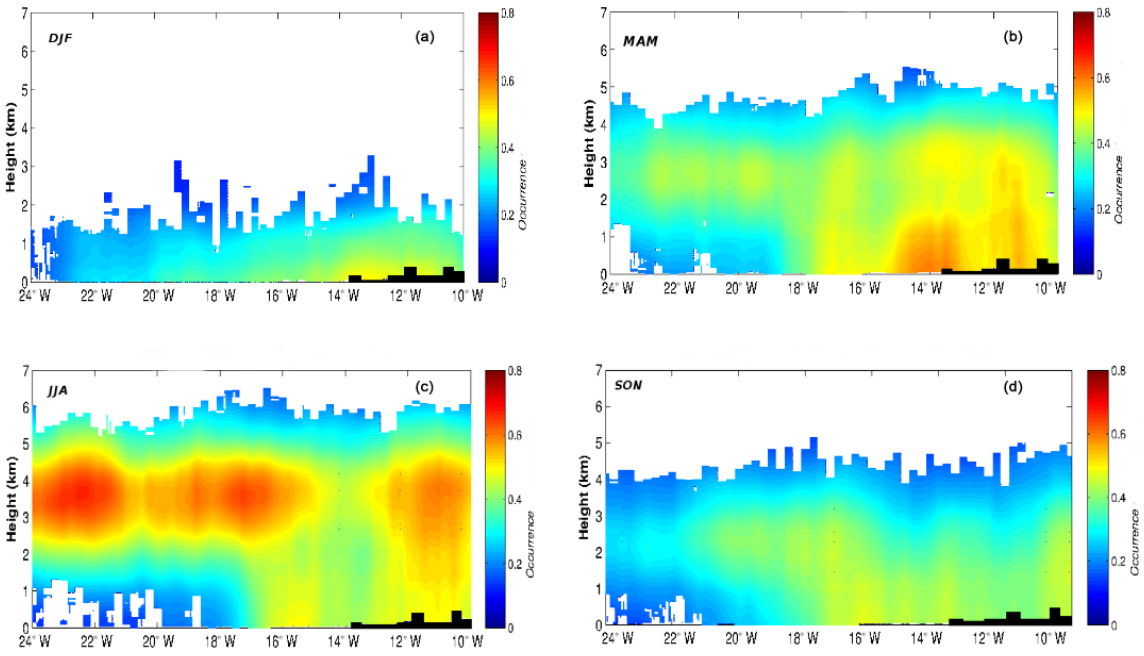

Figure 5. CALIOP daytime seasonal vertical distribution of the frequency of mineral dust aerosol occurrence zonally averaged between 12 and 21° N over the period 2007–2013: **(a)** DJF; **(b)** MAM; **(c)** JJA; and **(d)** SON.

nent (10–15° W). Above the ocean we see a detachment of the SAL from the ocean surface which occurs at the coast (around 18° W).

JJA is the busiest season of the year in terms of dust rising in the northern hemisphere of Africa. It is characterized by the development of density currents that intensify the mobilization of terrigenous aerosols (e.g., Bou Karam et al., 2008; Schepanski et al., 2009b, Fig. 5c). Unlike DJF, we note a clear separation of the dust layer above the eastern Atlantic Ocean where dusts are confined between 1 and 6 km altitude.

In SON, dust emissions decrease in intensity compared to JJA but the detachment from the surface of the ocean remains clear at the coast although less marked than in JJA (Fig. 5d). According to Adams et al. (2012), the heart of the SAL is located about 5 km above sea level in SON, whereas Liu et al. (2012) show a maximum altitude of 4 km.

4 Discussion

4.1 Seasonal variability

The desert aerosols in the band of latitude 12–21° N are mainly emitted in the Saharan and Sahelian regions. Emissions and transport processes are mainly controlled by meteorological variables (Brooks and Legrand, 2000; Joseph, 1999).

Schepanski et al. (2009b) found that over the Sahara sources of dust emissions are less active in winter than during summer. The southward migration of the Intertropical Convergence Zone (ITCZ) and the subsiding branch of the Hadley cell over the dry convection can also prevents the deep vertical distribution of aerosols in north Africa (Lavaysse et al., 2009). The maximum altitude of this distribution is 3 km above the continent and 2 km at the western African coast in agreement with the studies of Léon et al. (2009) and Vuolo et al. (2009). Compared to other seasons, DJF shows an important role played by the shallower atmospheric layers on the dust transported from source regions located in the northwestern part of Mauritania and more generally in coastal western Africa (Fig. 6a). This high occurrence is shown by the inter-seasonal variability derived from NCEP Reanalysis. Figure 6 highlights that the northwest region of Mauritania has the highest standard deviation of horizontal wind intensity between 18–24° N and that wind is very intense in winter compared to the other seasons (Fig. 6a). Hence this region represents an important sand source in winter as mentioned by previous studies (Bertrand et al., 1979; Ozer, 2000; Tulet et al., 2008; Laurent et al., 2008; Mokhtari, 2012; Hourdin et al., 2015).

Unlike winter, in summer as shown in Fig. 5c, dust is concentrated between the higher layers of the ABL, from 1 to 5–6 km (Gamo, 1996), in response to intense convective mechanisms that are more common in the region at this season (Cuesta et al., 2009). Indeed, the summer solar heating drives the development of the Saharan boundary layer which reaches up to 6 km while the convergence of hot dry air (Harmattan) from the Sahara with fresh moist air (monsoon) from the ocean generates intense convective cells which are responsible for the suspension of large amounts of dust which

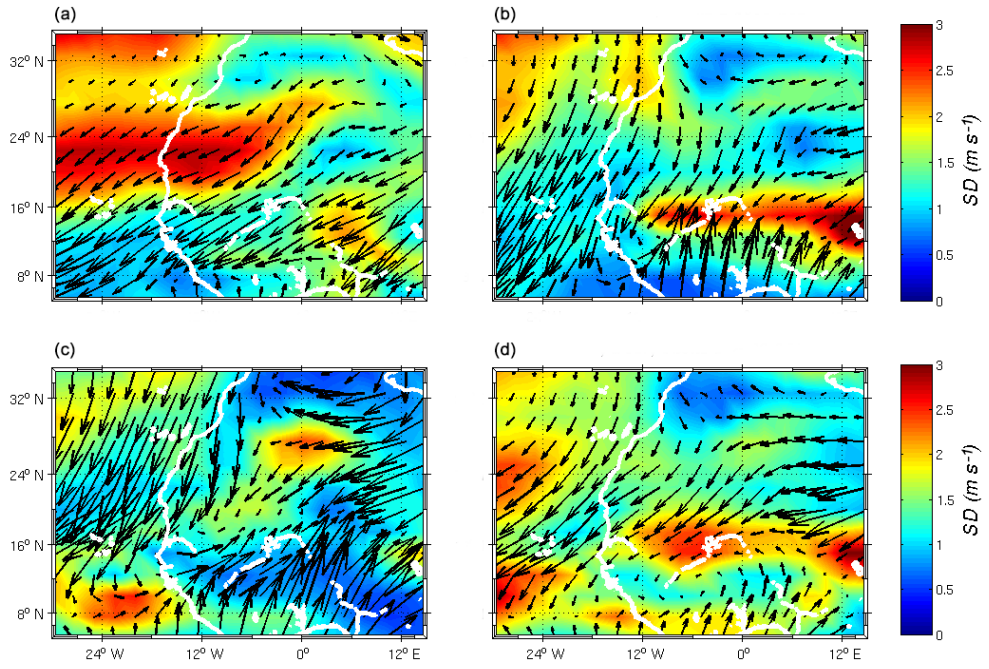

Figure 6. Seasonal mean zonal wind field at 925 hPa over western Africa from NCEP Reanalysis between 2000 and 2012: **(a)** DJF; **(b)** MAM; **(c)** JJA; and **(d)** SON. The vectors show wind direction while colors indicate the standard deviation of wind velocity ($m\,s^{-1}$).

will be distributed in the ABL. Transport also increases between 3 and 4 km above the ocean with a MDOF greater than 70 %, i.e., more than 30 % higher than that observed in DJF. This sharp increase of MDOF from DJF to JJA is in agreement with the results of Schepanski et al. (2009b), who estimated an increase of more than 20 % of the activity of dust sources in summer compared to winter in western Africa in the observations of Meteosat Second Generation (MSG) Spinning Enhanced Visible and Infrared Imager (SEVIRI). In summer, atmospheric dynamics raise large dust particles that are settling down much closer to the source regions than the rest of the year (Shao, 2000). However, their reflectivity of solar radiation becomes larger and reaches a maximum value indicated by a SSA of 0.97 (Fig. 4c).

In autumn, SSA values are comparable to spring values but these high values are not due to high reflectance of desert aerosols like in spring because the southern migration of the ITCZ reduces the activity of convective systems and causes a reduction of dust emissions shown by a decreasing of the AOD (Fig. 4d). These high SSA values can be attributed to atmospheric conditions seen through the relative humidity which is much higher than in spring (Fig. 7d). Indeed, OMI measures the atmospheric properties of the aerosols which are known to be hygroscopic (Jethva et al., 2014).

4.2 Continent–ocean transition

To better understand the factors responsible for the high variability of the vertical transition of desert aerosols from the continent to the ocean, we placed ourselves at a coastal point (Dakar) to study the variation of meteorological variables and their potential influence on the distribution of aerosols. Seasonality of vertical distributions of winds, relative humidity and potential temperature from radiosounding conducted at the weather station (GOOY) of Dakar (western African shore) are shown in Fig. 7.

In DJF, continental winds are very strong at the near-surface with a maximum of 25 $m\,s^{-1}$ at 500 m (Fig. 7a). The northeast direction of the winds in the first 1000 m explains the homogeneity of the vertical distribution of dust from the continent towards the ocean. This northeast wind applies to all western Africa at the surface (Fig. 6a). Their intensity also explain the strong values of MDOF (up to 50 %) observed by CALIOP in wintertime above the continent. Between 1 and 2 km height, winds weaken and change direction (south to southeast) while MDOF observed by satellite decreases (Fig. 5a). Between 2 and 5 km height, the winds turn to the southwest and west. These dust-depleted air masses of oceanic origin are wetter than from the land, and limit the development of the ABL. The air masses of continental origin are located between the surface and 2000 m height (Fig. 7a). In Fig. 7a, the relative humidity is around 20 % (between 500 and 2000 m) and it corresponds to a very dry air mass of Saharan origin. Between 2 and 5 km the potential temperature indicates a stable atmospheric layer. The DJF season is associated with an intermediate AOD value which decreases from 15° E to 10° W. SSA reflects mineral dust properties across its westward transportation (> 0.9), but it 0.2 higher over the ocean than the continent. We believe it could reflect

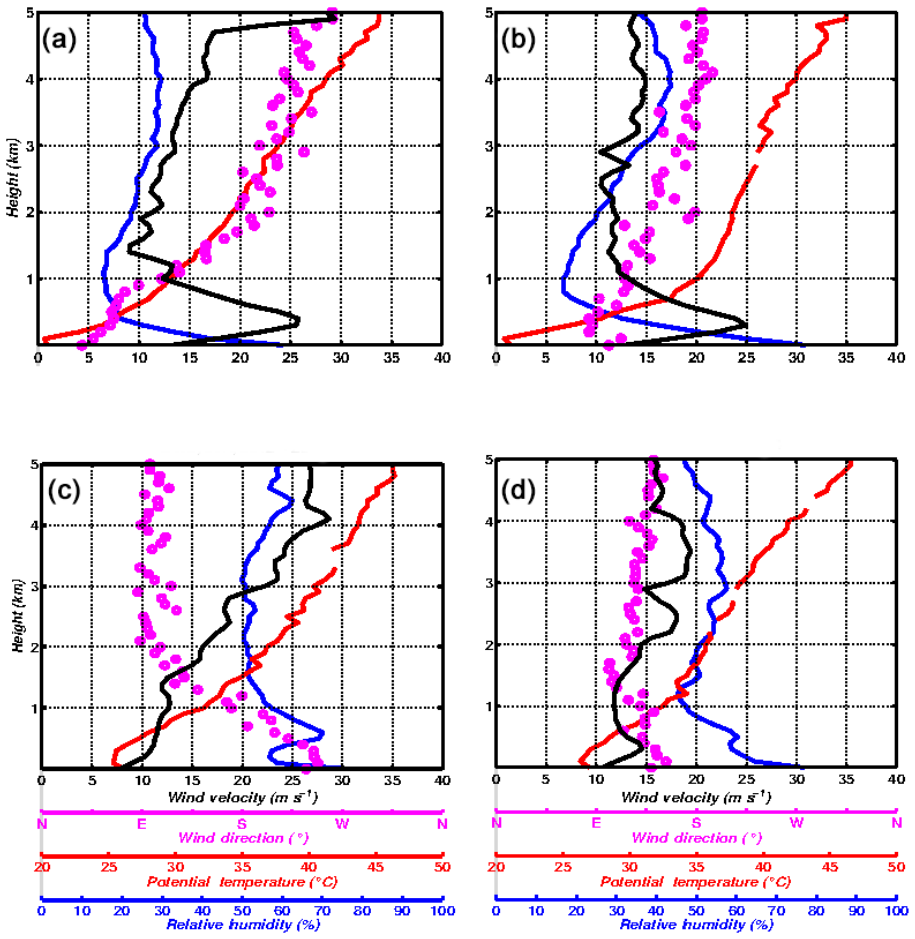

Figure 7. Mean seasonal vertical profiles of wind velocity (black line), wind direction (pink dots), potential temperature (red line), and relative humidity (blue line) at Dakar weather station (14.73° N, 17.51° W) for **(a)** DJF; **(b)** MAM; **(c)** JJA; and **(d)** SON. Observations correspond to weather balloons launched daily at 12:00 UTC for years 2012 to 2014.

the transport of dust emitted along the coastline which is only partly taken into account in dust properties derived from the continent.

Compared to the DJF situation, MAM near-surface winds (Fig. 7b) are still intense with a maximum of 25 m s^{-1} at 500 m height and are from the east. They are associated with MDOF above 50 % in the ABL around 14° W. Surface winds (Fig. 6b) indicate the near-surface convergence of northward and southward flows along 16° N which is associated with a well-mixed distribution of dust in the first 5 km of the atmosphere (Fig. 5b) and higher AOD values than in winter (Fig. 4). There is an inversion of easterly winds between 1 and 3 km and a second southerly wind peak (15 m s^{-1}) appears between 3 and 4 km. It corresponds to the dust layer (SAL) detected by CALIOP. The vertical profile of potential temperature indicates a stable thick layer, well mixed between the surface and 3 km (Fig. 7b). Beyond this altitude there is a stable stratification of the atmosphere indicated also by the potential temperature. Between 3 and 5 km height, the air masses coming from the south to the south-southwest are also of oceanic origin and their interaction with a more consistent amount of dust than in winter could explain the better marked transition between the ocean and the continent in terms of SSA (increase) and AOD (decrease) for this season (Fig. 4b). Indeed, in general, increasing the relative humidity is likely to increase the SSA and size hygroscopic aerosols with dry to wet passage inducing a larger diameter even when humidity is below the saturation level (Hervo, 2013; Howell et al., 2006).

In JJA, surface winds (0–1 km) decrease and are from the west to the southwest (West African Monsoon; Fig. 7c). This corresponds to lower values of MDOF (Fig. 5c) but to relative humidity values well above DJF or MAM (Fig. 7). Reid et al. (2002) presented a conceptual model of Saharan dust transport in the middle troposphere describing an evolution of relative humidity profile in agreement with the observations made in Dakar. These authors describe a moistening of the surface layers due to monsoon flow which penetrates up to 1.5 km above this layer. Figure 6c shows deep intrusion of air masses coming from the Gulf of Guinea which brings

humidity to the continent. The dry convection taking place over the continent favors the vertical transport of dust to high altitudes (Engelstaedter and Washington, 2007).

Between 2 and 6 km, winds are from the east and above 15 m s^{-1}. These wind velocity maxima reach 25 m s^{-1} in the range 3.5–5 km and are associated with the African easterly jet (AEJ) (Wu et al., 2009; Lafore et al., 2011). The co-localization of the AEJ and the SAL between 2 and 5 km height (Figs. 5c and 7c) causes the westward SAL transport by AEJ in summer (Karyampudi et al., 1999). These strong winds correspond to the layer of dust detected by satellite at this altitude (Fig. 5c). Above the continent, the mesoscale features associated with the convergence between Harmattan and the West African Monsoon at the ITCZ cause strong updrafts that allow lifting and transport of dust particles throughout the air column (Tulet et al., 2008). The dynamics of the monsoon described by the conceptual scheme of mechanisms controlling the dust vertical redistribution in Cuesta et al. (2009) explain the wide occurrence of dust found between 2 and 5 km rather than at the surface. During transport from northern Africa to the Atlantic Ocean, very large amounts of coarse dust (Fig. 4c) are deposited along the path with a rapid change in the size distribution of aerosols near the western African coast (Ryder et al., 2013). The changes of the aerosol size and properties will impact the climate system (Huneeus et al., 2011; Mahowald et al., 2014). McConnell et al. (2008) suggested that the variation in the aerosol profiles over the ocean have an impact on the radiative effect, a statement confirmed by Highwood et al. (2003), who showed that the radiative effect of mineral dust is correlated with the altitude of the dust layer.

The signing of the SAL is evidenced by relative dryness of the atmosphere (Dulac et al., 2001) between 1.5 and 5 km (Fig. 7c). At this altitude, the vertical profile of potential temperature indicates Saharan origin of air masses with temperatures between 35 and 45 °C (Carlson and Prospero, 1972). The wind direction (east) given in Fig. 7c between 1.5 and 5 km altitude confirms the origin of the Saharan air masses. The presence of dust in the SAL causes both warming and drying of the atmosphere between 1.5 and 5 km and a cooling below this layer (Tulet et al., 2008).

In SON, winds are weak and from the east at the surface (Figs. 7d and 6d). Between 1 and 5 km, it increases but is less intense than in JJA between 3 and 5 km and it is associated with a decrease of the MDOF (Fig. 5d). The moisture profile in SON (Fig. 7d) is close to that of JJA, but has a more humid atmosphere in the layer between 1.5 and 5 km where maximum relative humidity of the year occurs (60 %; Fig. 7d). The analysis of the vertical distribution of thermodynamic variables like relative humidity, potential temperature and wind measured at the Dakar weather station shows that the thermodynamical conditions control the dust vertical distribution as well as the depth of the dust layer depending on the season. This analysis also explains the unintuitive differences between spring, when the low values of SSA are associated with a strong AOD, and autumn, characterized by high values of SSA associated with low AOD values.

5 Conclusions

Studies of processes involved in the vertical distribution of aerosols at the transition between continent and ocean are very rare. Here, we took advantage of a weather station ideally located on the main pathway of desert aerosols from northern Africa (Léon et al., 2009; Marticorena et al., 2010; Mortier et al., 2016) to explain the effect of meteorological variables on this transition in a region of primary importance worldwide. The interaction of air masses of oceanic origin with dust aerosols are crucial for understanding their fate (e.g., Friese et al., 2016). This study constitutes the first attempt to link the seasonal dynamic of the atmosphere and the vertical distribution of dust aerosol in this region, and it provides the first dynamical explanation of a counterintuitive deposition pattern over the Atlantic Ocean. Indeed, it explains the role of the local atmospheric circulation in driving a higher AOD and dust content in summer over western Africa in phase with dust deposition in Barbados but in opposition with Cabo Verde islands where deposition is more intense in winter (Chiapello et al., 1995).

We have studied the seasonal variability of the distribution of desert aerosols in western Africa (continental and oceanic) from their optical and physical properties. First of all we have been able to show a good estimate of aerosol properties (AOD and SSA) of aerosols by satellite when compared with AERONET ground measurements on the mainland, the coast, and the ocean. Space observations then allowed us to show the predominant presence of Saharan dust in the atmosphere north of 12° N throughout the year and an additional significant contribution of sandy sources from the Mauritanian coast in winter. The MDOF indicates a change in the vertical distribution of dust at the transition between the continent and the ocean, the largest differences occurring in spring and summer seasons. In DJF, the ABL is shallow ($\sim$ 1 km) and strong winds from northeast transport the dust in a dry atmosphere from the continent to the ocean continuously. This surface layer is superimposed by a stable atmospheric layer which inhibits the vertical development of this surface layer rich in dust aerosols. The decrease from east to west of the AOD requires material deposition during the transit. In summer dry convection located north of 10° N and associated with structures that develop at the intertropical discontinuity (ITD) distribute dust up to 6 km height and create a thicker AOD. Above 6 km altitude over the Saharan and Sahelian regions, the vertical distribution of dust is blocked by the strong subsiding branch of the Hadley cell (Lavaysse et al., 2009). In the lower layers, the westward oceanic moistly entries which are opposite the higher eastward winds generate very different distributions above the continent and the ocean. On the mainland, the dust is domi-

nated by coarse mode and has a homogeneous vertical distribution, while above the ocean, lower layers are poor in dust and are superimposed by the SAL which is highly enriched. The SSA remains constant at this transition. MAM and SON represent transition periods. For the vertical dust distribution, MAM is closer to the summer situation.

Future modeling experiments should provide further insight into ocean–atmosphere processes involved in explaining this transition and the dust deposition along this pathway. It also seems that a more tailored approach to ocean–atmosphere interactions including higher frequencies of variability and notably the diurnal cycle is needed to make the role of local circulation on the vertical distribution of aerosols in coastal areas more apparent.

Data availability. All data links are provided below.

Radiosounding data were taken from http://weather.uwyo.edu/upperair/sounding.html. Two radiosoundings per day are launched at Dakar Airport (14.73° N, 17.5° W), providing weather data which are distributed by the Department of Atmospheric Science at the University of Wyoming.

The CALIPSO aerosol products are available at http://www.icare.univ-lille1.fr/archive. The CALIPSO data provide global coverage of the vertical distribution of the properties of clouds and aerosols.

NCEP Reanalysis data were found at http://www.esrl.noaa.gov/psd/data/gridded/data.ncep.reanalysis.pressure.html.

AERONET data sets are taken from http://aeronet.gsfc.nasa.gov/.

OMI data were obtained from NASA's Giovanni: http://disc.gsfc.nasa.gov/gesNews/giovanni_3_end_of_service?instance_id=omil2g&selectedMap=Blue%2520Marble&.

Competing interests. The authors declare that they have no conflict of interest.

Acknowledgements. We would like to thank the IRD-BMBF AWA project and the international joint laboratory ECLAIRS for supporting and promoting our research activities. We thank the Institute of Research for Development for funding this PhD study. We also thank ICARE for the online availability of the CALIPSO aerosol products at http://www.icare.univ-lille1.fr/archive. We are very grateful to Béatrice Marticorena and Isabelle Chiapello for very fruitful discussions. We are finally very grateful to the two anonymous referees for very informative comments which have greatly improved the quality of this study.

Edited by: Paola Formenti
Reviewed by: two anonymous referees

References

Adams, A. M., Prospero, J. M., and Zhang, C.: CALIPSO-derived three-dimensional structure of aerosol over the Atlantic Basin and adjacent continents, J. Climate, 25, 6862–6879, 2012.

Alizadeh-Choobari, O., Sturman, A., and Zawar-Reza, P.: A global satellite view of the seasonal distribution of mineral dust and its correlation with atmospheric circulation, Dynam. Atmos. Oceans, 68, 20–34, 2014.

Andreae, M. O.: Raising dust in the greenhouse, Nature, 380, 389–390, 1996.

Ansmann, A., Bösenberg, J., Chaikovsky, A., Comerón, A., Eckhardt, S., Eixmann, R., Freudenthaler, V., Ginoux, P., Komguem, L., Linné, H., Márquez, M. Á. L., Matthias, V., Mattis, I., Mitev, V., Müller, D., Music, S., Nickovic, S., Pelon, J., Sauvage, L., Sobolewsky, P., Srivastava, M. K., Stohl. A., Torres, O., Vaughan, G., Wandinger, U., and Wiegner M.: Long-range transport of Saharan dust to northern Europe: The 11–16 October 2001 outbreak observed with EARLINET, J. Geophys. Res.-Atmos., 108, 4783, https://doi.org/10.1029/2003JD003757, 2003.

Ansmann, A., Baars, H., Tesche, M., Müller, D., Althausen, D., Engelmann, R., Pauliquevis, T., and Artaxo, P.: Dust and smoke transport from Africa to South America: Lidar profiling over Cape Verde and the Amazon rainforest, Geophys. Res. Lett., 36, L11802, https://doi.org/10.1029/2009GL037923, 2009.

Arístegui, J., Barton, E. D., Álvarez-Salgado, X. A., Santos, A. M. P., Figueiras, F. G., Kifani, S., Hernández-León, S., Mason, E., Machú, E., and Demarcq, H.: Sub-regional ecosystem variability in the Canary Current upwelling, Prog. Oceanogr., 83, 33–48, 2009.

Baker, A., Kelly, S., Biswas, K., Witt, M., and Jickells, T.: Atmospheric deposition of nutrients to the Atlantic Ocean, Geophys. Res. Lett., 30, 2296, https://doi.org/10.1029/2003GL018518, 2003.

Ben-Ami, Y., Koren, I., and Altaratz, O.: Patterns of North African dust transport over the Atlantic: winter vs. summer, based on CALIPSO first year data, Atmos. Chem. Phys., 9, 7867–7875, https://doi.org/10.5194/acp-9-7867-2009, 2009.

Ben-Ami, Y., Koren, I., Rudich, Y., Artaxo, P., Martin, S. T., and Andreae, M. O.: Transport of North African dust from the Bodélé depression to the Amazon Basin: a case study, Atmos. Chem. Phys., 10, 7533–7544, https://doi.org/10.5194/acp-10-7533-2010, 2010.

Bergametti, G., Dutot, A.-L., Buat-Ménard, P., Losno, R., and Remoudaki, E.: Seasonal variability of the elemental composition of atmospheric aerosol particles over the northwestern Mediterranean, Tellus B, 41, 353–361, 1989.

Bertrand, J., Cerf, A., and Domergue, J.: Repartition in space and time of dust haze south of the Sahara, The Long-Range Transport of Pollutants and its Relation to Gen. Circulation Including Stratospheric/Tropospheric Exchange Processes, WMO 538, 409–415, 1979.

Bettenhausen, C. and Team, G. D. M.: Consistent Long-Term Aerosol Data Records over Land and Ocean from SeaWiFS, in: Goddard Space Flight Center Greenbelt, Maryland, 1–19, http://disc.sci.gsfc.nasa.gov/dust/documentation/README.DeepBlueSeaWiFS.pdf, 2013.

Bou Karam, D., Flamant, C., Knippertz, P., Reitebuch, O., Pelon, J., Chong, M., and Dabas, A.: Dust emissions over the Sahel associated with the West African monsoon intertropical discontinuity

region: A representative case-study, Q. J. Roy. Meteor. Soc., 134, 621–634, 2008.

Braun, S. A.: Reevaluating the role of the Saharan air layer in Atlantic tropical cyclogenesis and evolution, Mon. Weather Rev., 138, 2007–2037, 2010.

Brooks, N. and Legrand, M.: Dust variability over northern Africa and rainfall in the Sahel, in: Linking climate change to land surface change, 1–25, Springer, 2000.

Cakmur, R. V., Miller, R. L., and Tegen, I.: A comparison of seasonal and interannual variability of soil dust aerosols over the Atlantic Ocean as inferred by the TOMS AI and AVHRR AOT retrievals, J. Geophys. Res.-Atmos., 106, 18287–18303, 2001.

Carlson, T. N. and Prospero, J. M.: The large-scale movement of Saharan air outbreaks over the northern equatorial Atlantic, J. Appl. Meteorol., 11, 283–297, 1972.

Cavalieri, O., Cairo, F., Fierli, F., Di Donfrancesco, G., Snels, M., Viterbini, M., Cardillo, F., Chatenet, B., Formenti, P., Marticorena, B., and Rajot, J. L.: Variability of aerosol vertical distribution in the Sahel, Atmos. Chem. Phys., 10, 12005–12023, https://doi.org/10.5194/acp-10-12005-2010, 2010.

Chiapello, I. and Moulin, C.: TOMS and METEOSAT satellite records of the variability of Saharan dust transport over the Atlantic during the last two decades (1979–1997), Geophys. Res. Lett., 29, 1176, https://doi.org/10.1029/2001GL013767, 2002.

Chiapello, I., Bergametti, G., Gomes, L., Chatenet, B., Dulac, F., Pimenta, J., and Santos Suares, E.: An additional low layer transport of Sahelian and Saharan dust over the north-eastern tropical Atlantic, Geophys. Res. Lett., 22, 3191–3194, 1995.

Chiapello, I., Prospero, J., Herman, J., and Hsu, N.: Detection of mineral dust over the North Atlantic Ocean and Africa with the Nimbus 7 TOMS, J. Geophys. Res.-Atmos., 104, 9277–9291, 1999.

Chou, C., Formenti, P., Maille, M., Ausset, P., Helas, G., Osborne, S., and Harrison, M.: Size distribution, shape and composition of dust aerosols collected during the AMMA SOP0 field campaign in the northeast of Niger, January 2006, J. Geophys. Res, 113, D00C10, https://doi.org/10.1029/2008JD009897, 2008.

Claquin, T., Schulz, M., and Balkanski, Y.: Modeling the mineralogy of atmospheric dust sources, J. Geophys. Res.-Atmos., 104, 22243–22256, 1999.

Cuesta, J., Marsham, J. H., Parker, D. J., and Flamant, C.: Dynamical mechanisms controlling the vertical redistribution of dust and the thermodynamic structure of the West Saharan atmospheric boundary layer during summer, Atmos. Sci. Lett., 10, 34–42, 2009.

Diokhane, A. M., Jenkins, G. S., Manga, N., Drame, M. S., and Mbodji, B.: Linkages between observed, modeled Saharan dust loading and meningitis in Senegal during 2012 and 2013, Int. J. Biometeorol., 60, 557–575, 2016.

Dubovik, O., Smirnov, A., Holben, B., King, M., Kaufman, Y., Eck, T., and Slutsker, I.: Accuracy assessments of aerosol optical properties retrieved from Aerosol Robotic Network (AERONET) Sun and sky radiance measurements, J. Geophys. Res.-Atmos., 105, 9791–9806, 2000.

Dubovik, O., Holben, B., Eck, T. F., Smirnov, A., Kaufman, Y. J., King, M. D., Tanré, D., and Slutsker, I.: Variability of absorption and optical properties of key aerosol types observed in worldwide locations, J. Atmos. Sci., 59, 590–608, 2002.

Duce, R. A. and Tindale, N. W.: Atmospheric transport of iron and its deposition in the ocean, Limnol. Oceanogr., 36, 1715–1726, 1991.

Dulac, F., Chazette, P., Gomes, L., Chatenet, B., Berger, H., and Dos Santos, J. V.: A method for aerosol profiling in the lower troposphere with coupled scatter and meteorological rawindsondes and first data from the tropical Atlantic off Sahara, J. Aerosol Sci., 32, 1069–1086, 2001.

Dunion, J. P. and Marron, C. S.: A reexamination of the Jordan mean tropical sounding based on awareness of the Saharan air layer: Results from 2002, J. Climate, 21, 5242–5253, 2008.

Eck, T. F., Holben, B. N., Reid, J. S., Dubovick, O., Smirnov, A., O'Neil, N. T., Slutsker, I., and Kinne, S.: Wavelength dependence of the optical depth of biomass burning, urban, and desert dust aerosols, J. Geophys. Res., 104, 31333–31349, 1999.

Engelstaedter, S. and Washington, R.: Atmospheric controls on the annual cycle of North African dust, J. Geophys. Res.-Atmos., 112, D03103, https://doi.org/10.1029/2006JD007195, 2007.

Engelstaedter, S., Tegen, I., and Washington, R.: North African dust emissions and transport, Earth-Sci. Rev., 79, 73–100, 2006.

Eplee, R. E., Patt, F. S., Barnes, R. A., and McClain, C. R.: SeaWiFS long-term solar diffuser reflectance and sensor noise analyses, Appl. Optics, 46, 762–773, 2007.

Eplee Jr., R. E., Sun, J.-Q., Meister, G., Patt, F. S., Xiong, X., and McClain, C. R.: Cross calibration of SeaWiFS and MODIS using on-orbit observations of the Moon, Appl. Optics, 50, 120–133, 2011.

Formenti, P., Andreae, M., Lange, L., Roberts, G., Cafmeyer, J., Rajta, I., Maenhaut, W., Holben, B., Artaxo, P., and Lelieveld, J.: Saharan dust in Brazil and Suriname during the Large-Scale Biosphere-Atmosphere Experiment in Amazonia (LBA)-Cooperative LBA Regional Experiment (CLAIRE) in March 1998, J. Geophys. Res.-Atmos., 106, 14919–14934, 2001.

Formenti, P., Rajot, J. L., Desboeufs, K., Caquineau, S., Chevaillier, S., Nava, S., Gaudichet, A., Journet, E., Triquet, S., Alfaro, S., Chiari, M., Haywood, J., Coe, H., and Highwood, E.: Regional variability of the composition of mineral dust from western Africa: Results from the AMMA SOP0/DABEX and DODO field campaigns, J. Geophys. Res.-Atmos., 113, D00C13, https://doi.org/10.1029/2008JD009903, 2008.

Franz, B. A., Bailey, S. W., Werdell, P. J., and McClain, C. R.: Sensor-independent approach to the vicarious calibration of satellite ocean color radiometry, Appl. Optics, 46, 5068–5082, 2007.

Friese, C. A., van der Does, M., Merkel, U., Iversen, M. H., Fischer, G., and Stuut, J.-B. W.: Environmental factors controlling the seasonal variability in particle size distribution of modern Saharan dust deposited off Cape Blanc, Aeolian Research, 22, 165–179, 2016.

Gamo, M.: Thickness of the dry convection and large-scale subsidence above deserts, Bound.-Lay. Meteorol., 79, 265–278, 1996.

Ganor, E. and Mamane, Y.: Transport of Saharan dust across the eastern Mediterranean, Atmos. Environ., 16, 581–587, 1982.

Ganor, E., Osetinsky, I., Stupp, A., and Alpert, P.: Increasing trend of African dust, over 49 years, in the eastern Mediterranean, J. Geophys. Res.-Atmos., 115, D07201, https://doi.org/10.1029/2009JD012500, 2010.

Generoso, S., Bey, I., Labonne, M., and Bréon, F.-M.: Aerosol vertical distribution in dust outflow over the Atlantic: Comparisons

between GEOS-Chem and Cloud-aerosol Lidar and Infrared Pathfinder Satellite Observation (CALIPSO), J. Geophys. Res.-Atmos., 113, D24209, https://doi.org/10.1029/2008JD010154, 2008.

Griffin, D. W.: Atmospheric movement of microorganisms in clouds of desert dust and implications for human health, Clin. Microbiol. Rev., 20, 459–477, 2007.

Heese, B. and Wiegner, M.: Vertical aerosol profiles from Raman polarization lidar observations during the dry season AMMA field campaign, J. Geophys. Res.-Atmos., 113, D00C11, https://doi.org/10.1029/2007JD009487, 2008.

Hervo, M.: Etude des propriétés optiques et radiatives des aérosols en atmosphère réelle: Impact de l'hygroscopicité, PhD thesis, Université Blaise Pascal-Clermont-Ferrand II, 2013.

Highwood, E. J., Haywood, J. M., Silverstone, M. D., Newman, S. M., and Taylor, J. P.: Radiative properties and direct effect of Saharan dust measured by the C-130 aircraft during Saharan Dust Experiment (SHADE): 2. Terrestrial spectrum, J. Geophys. Res.-Atmos., 108, 8578, https://doi.org/10.1029/2002JD002552, 2003.

Holben, B., Tanre, D., Smirnov, A., Eck, T., Slutsker, I., Abuhassan, N., Newcomb, W., Schafer, J., Chatenet, B., Lavenu, F., Kaufman, Y. J., Vande Castle, J., Setzer, A., Markham, B., Clark, D., Frouin, R., Halthore, R., Karneli, A., O'Neill, N. T., Pietras, C., Pinker, R. T., Voss, K., and Zibordi, G.: An emerging ground-based aerosol climatology: Aerosol optical depth from AERONET, J. Geophys. Res.-Atmos., 106, 12067–12097, 2001.

Holben, B. N., Eck, T., Slutsker, I., Tanre, D., Buis, J., Setzer, A., Vermote, E., Reagan, J. A., Kaufman, Y., Nakajima, T., Lavenu, F., Jankowiak, I., and Smirnov, A.: AERONET – A federated instrument network and data archive for aerosol characterization, Remote Sens. Environ., 66, 1–16, 1998.

Hourdin, F., Gueye, M., Diallo, B., Dufresne, J.-L., Escribano, J., Menut, L., Marticoréna, B., Siour, G., and Guichard, F.: Parameterization of convective transport in the boundary layer and its impact on the representation of the diurnal cycle of wind and dust emissions, Atmos. Chem. Phys., 15, 6775–6788, https://doi.org/10.5194/acp-15-6775-2015, 2015.

Howell, S., Clarke, A., Shinozuka, Y., Kapustin, V., McNaughton, C., Huebert, B., Doherty, S., and Anderson, T.: Influence of relative humidity upon pollution and dust during ACE-Asia: Size distributions and implications for optical properties, J. Geophys. Res.-Atmos., 111, D06205, https://doi.org/10.1029/2004JD005579, 2006.

Hsu, N. C., Gautam, R., Sayer, A. M., Bettenhausen, C., Li, C., Jeong, M. J., Tsay, S.-C., and Holben, B. N.: Global and regional trends of aerosol optical depth over land and ocean using SeaWiFS measurements from 1997 to 2010, Atmos. Chem. Phys., 12, 8037–8053, https://doi.org/10.5194/acp-12-8037-2012, 2012.

Hsu, N. C., Tsay, S.-C., King, M. D., and Herman, J. R.: Aerosol properties over bright-reflecting source regions, IEEE T. Geosci. Remote Sens., 42, 557–569, 2004.

Huneeus, N., Schulz, M., Balkanski, Y., Griesfeller, J., Prospero, J., Kinne, S., Bauer, S., Boucher, O., Chin, M., Dentener, F., Diehl, T., Easter, R., Fillmore, D., Ghan, S., Ginoux, P., Grini, A., Horowitz, L., Koch, D., Krol, M. C., Landing, W., Liu, X., Mahowald, N., Miller, R., Morcrette, J.-J., Myhre, G., Penner, J., Perlwitz, J., Stier, P., Takemura, T., and Zender, C. S.: Global dust model intercomparison in AeroCom phase I, Atmos. Chem. Phys., 11, 7781–7816, https://doi.org/10.5194/acp-11-7781-2011, 2011.

Hunt, W. H., Winker, D. M., Vaughan, M. A., Powell, K. A., Lucker, P. L., and Weimer, C.: CALIPSO lidar description and performance assessment, J. Atmos. Ocean. Tech., 26, 1214–1228, 2009.

Ialongo, I., Buchard, V., Brogniez, C., Casale, G. R., and Siani, A. M.: Aerosol Single Scattering Albedo retrieval in the UV range: an application to OMI satellite validation, Atmos. Chem. Phys., 10, 331–340, https://doi.org/10.5194/acp-10-331-2010, 2010.

Israelevich, P., Ganor, E., Levin, Z., and Joseph, J.: Annual variations of physical properties of desert dust over Israel, J. Geophys. Res.-Atmos., 108, 4381, https://doi.org/10.1029/2002JD003163, 2003.

Jamet, C., Moulin, C., and Thiria, S.: Monitoring aerosol optical properties over the Mediterranean from SeaWiFS images using a neural network inversion, Geophys. Res. Lett., 31, L13107, https://doi.org/10.1029/2004GL019951, 2004.

Jethva, H., Torres, O., and Ahn, C.: Global assessment of OMI aerosol single-scattering albedo using ground-based AERONET inversion, J. Geophys. Res.-Atmos., 119, 9020–9040, 2014.

Jickells, T., An, Z., Andersen, K. K., Baker, A., Bergametti, G., Brooks, N., Cao, J., Boyd, P., Duce, R., Hunter, K., Kawahata, K., Kulibay, N., laRoche, J., Liss, P., Mahowald, N., Prospero, J., Ridgwell, A., Tegen, I., and Torres, R.: Global iron connections between desert dust, ocean biogeochemistry, and climate, Science, 308, 67–71, 2005.

Johnson, B. and Osborne, S.: Physical and optical properties of mineral dust aerosol measured by aircraft during the GERBILS campaign, Q. J. Roy. Meteor. Soc., 137, 1117–1130, 2011.

Johnson, B., Osborne, S., Haywood, J., and Harrison, M.: Aircraft measurements of biomass burning aerosol over West Africa during DABEX, J. Geophys. Res.-Atmos., 113, D00C06, https://doi.org/10.1029/2007JD009451, 2008.

Joseph, M.: Long-term measurements of the transport of African mineral dust to the southeastern United States: Implications for regional air quality, 104, 15917–15927, 1999.

Karyampudi, V. M., Palm, S. P., Reagen, J. A., Fang, H., Grant, W. B., Hoff, R. M., Moulin, C., Pierce, H. F., Torres, O., Browell, E. V., and Melfi, S. H.: Validation of the Saharan dust plume conceptual model using lidar, Meteosat, and ECMWF data, B. Am. Meteorol. Soc., 80, 1045, https://doi.org/10.1175/1520-0477, 1999.

Kaufman, Y., Koren, I., Remer, L., Tanré, D., Ginoux, P., and Fan, S.: Dust transport and deposition observed from the Terra-Moderate Resolution Imaging Spectroradiometer (MODIS) spacecraft over the Atlantic Ocean, J. Geophys. Res.-Atmos., 110, D10S12, https://doi.org/10.1029/2003JD004436, 2005.

Lafore, J.-P., Flamant, C., Guichard, F., Parker, D., Bouniol, D., Fink, A., Giraud, V., Gosset, M., Hall, N., Höller, H., Jones, S. C., Protat, A., Roca, R., Roux, F., Saïd, F., and Thomcroft, C.: Progress in understanding of weather systems in West Africa, Atmos. Sci. Lett., 12, 7–12, 2011.

Laurent, B., Marticorena, B., Bergametti, G., Léon, J., and Mahowald, N.: Modeling mineral dust emissions from the Sahara desert using new surface properties and soil database, J. Geophys. Res.-Atmos., 113, D14218, https://doi.org/10.1029/2007JD009484, 2008.

Lavaysse, C., Flamant, C., Janicot, S., Parker, D., Lafore, J.-P., Sultan, B., and Pelon, J.: Seasonal evolution of the West African heat low: a climatological perspective, Clim. Dynam., 33, 313–330, 2009.

Léon, J.-F., Derimian, Y., Chiapello, I., Tanré, D., Podvin, T., Chatenet, B., Diallo, A., and Deroo, C.: Aerosol vertical distribution and optical properties over M'Bour (16.96° W; 14.39° N), Senegal from 2006 to 2008, Atmos. Chem. Phys., 9, 9249–9261, https://doi.org/10.5194/acp-9-9249-2009, 2009.

Levelt, P. F., van den Oord, G. H., Dobber, M. R., Malkki, A., Visser, H., de Vries, J., Stammes, P., Lundell, J. O., and Saari, H.: The ozone monitoring instrument, IEEE T. Geosci. Remote Sens., 44, 1093–1101, 2006.

Liu, D., Wang, Z., Liu, Z., Winker, D., and Trepte, C.: A height resolved global view of dust aerosols from the first year CALIPSO lidar measurements, J. Geophys. Res.-Atmos., 113, D16214, https://doi.org/10.1029/2007JD009776, 2008.

Liu, D., Wang, Y., Wang, Z., and Zhou, J.: The three-dimensional structure of transatlantic African dust transport: a new perspective from CALIPSO LIDAR measurements, Adv. Meteorol., 2012, 850704, https://doi.org/10.1155/2012/850704, 2012.

Liu, Z., Omar, A., Hu, Y., Vaughan, M., Winker, D., Poole, L., and Kovacs, T.: CALIOP algorithm theoretical basis document. Part 3: Scene classification algorithms, NASA-CNES document PC-SCI-203, 2005.

Mahowald, N., Albani, S., Kok, J. F., Engelstaeder, S., Scanza, R., Ward, D. S., and Flanner, M. G.: The size distribution of desert dust aerosols and its impact on the Earth system, Aeolian Research, 15, 53–71, 2014.

Mahowald, N. M., Engelstaedter, S., Luo, C., Sealy, A., Artaxo, P., Benitez-Nelson, C., Bonnet, S., Chen, Y., Chuang, P. Y., Cohen, D. D., Dulac, F., Herut, B., Johansen, A., M., Kulibay, N., Losno, R., Maenhaut, W., Paytan, A., Prospero, J. M., Shank, L. M., and Siefert, R. L.: Atmospheric Iron Deposition: Global Distribution, Variability, and Human Perturbations*, Annual Review of Marine Science, 1, 245–278, 2009.

Malavelle, F.: Effets direct et semi-direct des aérosols en Afrique de l'ouest pendant la saison sèche, PhD thesis, Université Paul Sabatier-Toulouse III, 2011.

Marticorena, B., Chatenet, B., Rajot, J. L., Traoré, S., Coulibaly, M., Diallo, A., Koné, I., Maman, A., NDiaye, T., and Zakou, A.: Temporal variability of mineral dust concentrations over West Africa: analyses of a pluriannual monitoring from the AMMA Sahelian Dust Transect, Atmos. Chem. Phys., 10, 8899–8915, https://doi.org/10.5194/acp-10-8899-2010, 2010.

Martin, J. H.: Iron as a limiting factor in oceanic productivity, in: Primary productivity and biogeochemical cycles in the sea, 123–137, Springer, 1992.

Martiny, N. and Chiapello, I.: Assessments for the impact of mineral dust on the meningitis incidence in West Africa, Atmos. Environ., 70, 245–253, 2013.

McConnell, C., Highwood, E., Coe, H., Formenti, P., Anderson, B., Osborne, S., Nava, S., Desboeufs, K., Chen, G., and Harrison, M.: Seasonal variations of the physical and optical characteristics of Saharan dust: Results from the Dust Outflow and Deposition to the Ocean (DODO) experiment, J. Geophys. Res.-Atmos., 113, D14S05, https://doi.org/10.1029/2007JD009606, 2008.

Messager, C., Parker, D. J., Reitebuch, O., Agusti-Panareda, A., Taylor, C. M., and Cuesta, J.: Structure and dynamics of the Saharan atmospheric boundary layer during the West African monsoon onset: Observations and analyses from the research flights of 14 and 17 July 2006, Q. J. Roy. Meteor. Soc., 136, 107–124, 2010.

Mielonen, T., Arola, A., Komppula, M., Kukkonen, J., Koskinen, J., de Leeuw, G., and Lehtinen, K.: Comparison of CALIOP level 2 aerosol subtypes to aerosol types derived from AERONET inversion data, Geophys. Res. Lett., 36, L18804, https://doi.org/10.1029/2009GL039609, 2009.

Mills, M. M., Ridame, C., Davey, M., La Roche, J., and Geider, R. J.: Iron and phosphorus co-limit nitrogen fixation in the eastern tropical North Atlantic, Nature, 429, 292–294, 2004.

Mokhtari, M.: Amélioration de la prise en compte des aérosols terrigènes dans les modèles atmosphériques à moyenne échelle, PhD thesis, Université de Toulouse, Université Toulouse III-Paul Sabatier, 2012.

Mortier, A., Goloub, P., Derimian, Y., Tanré, D., Podvin, T., Blarel, L., Deroo, C., Marticorena, B., Diallo, A., and Ndiaye, T.: Climatology of aerosol properties and clear-sky shortwave radiative effects using Lidar and Sun photometer observations in the Dakar site, J. Geophys. Res.-Atmos., 121, https://doi.org/10.1002/2015JD024588, 2016.

Moulin, C.: Transport atmosphérique des poussières africaines sur la Méditerranée et l'Atlantique: climatologie satellitale à partir des images Météosat VIS(1983-1994) et relations avec le climat, PhD thesis, 1997.

Omar, A. H., Winker, D. M., Vaughan, M. A., Hu, Y., Trepte, C. R., Ferrare, R. A., Lee, K.-P., Hostetler, C. A., Kittaka, C., Rogers, R. R., Liu, Z., and Kuehn, R. E.: The CALIPSO automated aerosol classification and lidar ratio selection algorithm, J. Atmos. Ocean. Tech., 26, 1994–2014, 2009.

Ozer, P.: Les lithométéores en région sahélienne: un indicateur climatique de la désertification, Ph.D. thesis, Université de Liège Faculté des sciences Liège Belgique, Liège, Belgique, 2000.

Petzold, A., Veira, A., Mund, S., Esselborn, M., Kiemle, C., Weinzierl, B., Hamburger, T., Ehret, G., Lieke, K., and Kandler, K.: Mixing of mineral dust with urban pollution aerosol over Dakar (Senegal): impact on dust physico-chemical and radiative properties, Tellus B, 63, 619–634, 2011.

Prospero, J., Glaccum, R., and Nees, R.: Atmospheric transport of soil dust from Africa to South America, Nature, 289, 570–572, 1981.

Prospero, J. M., Blades, E., Mathison, G., and Naidu, R.: Interhemispheric transport of viable fungi and bacteria from Africa to the Caribbean with soil dust, Aerobiologia, 21, 1–19, 2005.

Ramanathan, V., Crutzen, P., Kiehl, J., and Rosenfeld, D.: Aerosols, climate, and the hydrological cycle, Science, 294, 2119–2124, 2001.

Reid, J. S., Westphal, D. L., Livingston, J. M., Savoie, D. L., Maring, H. B., Jonsson, H. H., Eleuterio, D. P., Kinney, J. E., and Reid, E. A.: Dust vertical distribution in the Caribbean during the Puerto Rico Dust Experiment, Geophys. Res. Lett., 29, 1151, https://doi.org/10.1029/2001GL014092, 2002.

Ridley, D., Heald, C., and Ford, B.: North African dust export and deposition: A satellite and model perspective, J. Geophys. Res.-Atmos., 117, D02202, https://doi.org/10.1029/2011JD016794, 2012.

Ryder, C., Highwood, E., Lai, T., Sodemann, H., and Marsham, J.: Impact of atmospheric transport on the evolution of microphys-

ical and optical properties of Saharan dust, Geophys. Res. Lett., 40, 2433–2438, 2013.

Sayer, A., Hsu, N., Bettenhausen, C., Ahmad, Z., Holben, B., Smirnov, A., Thomas, G., and Zhang, J.: SeaWiFS Ocean Aerosol Retrieval (SOAR): Algorithm, validation, and comparison with other data sets, J. Geophys. Res.-Atmos., 117, D03206, https://doi.org/10.1029/2011JD016599, 2012.

Schepanski, K., Tegen, I., Laurent, B., Heinold, B., and Macke, A.: A new Saharan dust source activation frequency map derived from MSG-SEVIRI IR-channels, Geophys. Res. Lett., 34, L18803, https://doi.org/10.1029/2007GL030168, 2007.

Schepanski, K., Tegen, I., and Macke, A.: Saharan dust transport and deposition towards the tropical northern Atlantic, Atmos. Chem. Phys., 9, 1173–1189, https://doi.org/10.5194/acp-9-1173-2009, 2009a.

Schepanski, K., Tegen, I., Todd, M., Heinold, B., Bönisch, G., Laurent, B., and Macke, A.: Meteorological processes forcing Saharan dust emission inferred from MSG-SEVIRI observations of subdaily dust source activation and numerical models, J. Geophys. Res.-Atmos., 114, D10201, https://doi.org/10.1029/2008JD010325, 2009b.

Schepanski, K., Tegen, I., and Macke, A.: Comparison of satellite based observations of Saharan dust source areas, Remote Sens. Environ., 123, 90–97, 2012.

Shao, Y.: Physics and modelling of wind erosion (atmospheric and oceanographic sciences library), vol. 37, Springer Science & Business Media, 2000.

Sokolik, I. N. and Toon, O. B.: Incorporation of mineralogical composition into models of the radiative properties of mineral aerosol from UV to IR wavelengths, J. Geophys. Res., 104, 9423–9444, 1999.

Solomon, S.: Climate change 2007-the physical science basis: Working group I contribution to the fourth assessment report of the IPCC, vol. 4, Cambridge University Press, 2007.

Stith, J., Ramanathan, V., Cooper, W., Roberts, G., DeMott, P., Carmichael, G., Hatch, C., Adhikary, B., Twohy, C., Rogers, D., Baumgardner, D., Prenni, A. J., Campos, T., Gao, R., Anderson, J., and Feng, Y.: An overview of aircraft observations from the Pacific Dust Experiment campaign, J. Geophys. Res.-Atmos., 114, D05207, https://doi.org/10.1029/2008JD010924, 2009.

Swap, R., Garstang, M., Greco, S., Talbot, R., and Kållberg, P.: Saharan dust in the Amazon Basin, Tellus B, 44, 133–149, 1992.

Taghavi, F. and Asadi, A.: The Persian Gulf 12th April 2007 dust storm: observation and model analysis, in: EUMETSAT Meteorological Satellite Conference, Darmstadt, Germany, 8–12, 2008.

Tanaka, T. Y., Kurosaki, Y., Chiba, M., Matsumura, T., Nagai, T., Yamazaki, A., Uchiyama, A., Tsunematsu, N., and Kai, K.: Possible transcontinental dust transport from North Africa and the Middle East to East Asia, Atmos. Environ., 39, 3901–3909, 2005.

Tegen, I., Schepanski, K., and Heinold, B.: Comparing two years of Saharan dust source activation obtained by regional modelling and satellite observations, Atmos. Chem. Phys., 13, 2381–2390, https://doi.org/10.5194/acp-13-2381-2013, 2013.

Teller, A. and Levin, Z.: The effects of aerosols on precipitation and dimensions of subtropical clouds: a sensitivity study using a numerical cloud model, Atmos. Chem. Phys., 6, 67–80, https://doi.org/10.5194/acp-6-67-2006, 2006.

Thomson, M. C., Molesworth, A. M., Djingarey, M. H., Yameogo, K., Belanger, F., and Cuevas, L. E.: Potential of environmental models to predict meningitis epidemics in Africa, Trop. Med. Int. Health, 11, 781–788, 2006.

Tsamalis, C., Chédin, A., Pelon, J., and Capelle, V.: The seasonal vertical distribution of the Saharan Air Layer and its modulation by the wind, Atmos. Chem. Phys., 13, 11235–11257, https://doi.org/10.5194/acp-13-11235-2013, 2013.

Tulet, P., Mallet, M., Pont, V., Pelon, J., and Boone, A.: The 7–13 March 2006 dust storm over West Africa: Generation, transport, and vertical stratification, J. Geophys. Res.-Atmos., 113, D00C08, https://doi.org/10.1029/2008JD009871, 2008.

Vuolo, M. R., Chepfer, H., Menut, L., and Cesana, G.: Comparison of mineral dust layers vertical structures modeled with CHIMERE-DUST and observed with the CALIOP lidar, J. Geophys. Res.-Atmos., 114, D09214, https://doi.org/10.1029/2008JD011219, 2009.

Wagener, T.: Le fer à l'interface océan-atmosphère: Flux et processus de dissolution dans l'eau de mer., PhD thesis, Université de la Méditerranée-Aix-Marseille II, 2008.

Wang, M., Bailey, S., Pietras, C., McClain, C., and Riley, T.: SeaWiFS aerosol optical thickness matchup analyses, The Sea-WiFS Postlaunch Technical Report Series, 10, 39–44, 2000.

Weinzierl, B., Ansmann, A., Prospero, J., Althausen, D., Benker, N., Chouza, F., Dollner, M., Farrell, D., Fomba, W., Freudenthaler, V., Gasteiger, J., Groß, S., Haarig, M., Heinold, B., Kandler, K., Kristensen, T. B., Mayol-Bracero, O. L., Müller, T., Reitebuch, O., Sauer, D., Schäfler, A., Schepanski, K., Spanu, A., Tegen, I., Toledano, C., and Walser, A.: The Saharan Aerosol Long-range Transport and Aerosol-Cloud-Interaction Experiment (SALTRACE): overview and selected highlights, B. Am. Meteorol. Soc., https://doi.org/10.1175/BAMS-D-15-00142.1, 2016.

Winker, D.: Accounting for multiple scattering in retrievals from space lidar, in: Proc. of SPIE Vol, vol. 5059, p. 129, 2003.

Winker, D. M., Hostetler, C., Vaughan, M., and Omar, A.: CALIOP Algorithm Theoretical Basis Document, Part 1: CALIOP Instrument, and Algorithms Overview, Release, J. Atmos. Ocean. Tech., 26, 2310–2323, 2006.

Winker, D. M., Hunt, W. H., and McGill, M. J.: Initial performance assessment of CALIOP, Geophys. Res. Lett., 34, L19803, https://doi.org/10.1029/2007GL030135, 2007.

Wu, M.-L. C., Reale, O., Schubert, S. D., Suarez, M. J., Koster, R. D., and Pegion, P. J.: African easterly jet: structure and maintenance, J. Climate, 22, 4459–4480, 2009.

Yang, W., Marshak, A., Várnai, T., Kalashnikova, O. V., and Kostinski, A. B.: CALIPSO observations of transatlantic dust: vertical stratification and effect of clouds, Atmos. Chem. Phys., 12, 11339–11354, https://doi.org/10.5194/acp-12-11339-2012, 2012.

Yu, H., Chin, M., Winker, D. M., Omar, A. H., Liu, Z., Kittaka, C., and Diehl, T.: Global view of aerosol vertical distributions from CALIPSO lidar measurements and GOCART simulations: Regional and seasonal variations, J. Geophys. Res.-Atmos., 115, D00H30, https://doi.org/10.1029/2009JD013364, 2010.